

Supporting Information

Label-free G-quadruplex aptamer fluorescent aptasensor for visual and real-time kanamycin detection in the lake and human samples

Yingnan Ma^a, Gang Shen^{b*}, Runzhi Li^a, Changzheng Wang^{a*}, Fengmin Yang^b, Fangfang Wang^b, Huanfeng Ye^b, Hong Zhang^{b*}, Yalin Tang^{b,c*}

^a Key Laboratory of Urban Stormwater System and Water Environment, Ministry of Education, Beijing University of Civil Engineering and Architecture, Beijing 100044, China

^b National Laboratory for Molecular Sciences, Center for Molecular Sciences, State Key Laboratory for Structural Chemistry of Unstable and Stable Species, Institute of Chemistry Chinese Academy of Sciences, Beijing 100190, China

^c University of Chinese Academy of Sciences, Beijing 100049, China

* Corresponding authors

E-mail: sg2009@iccas.ac.cn, zhanghong@iccas.ac.cn, wcz@bucea.edu.cn, tangyl@iccas.ac.cn

Fax: 0086-10-8261-7302

Tel: 0086-10-6256-3101

Table of content

MS-ESI spectrum of CyT -----	S3
¹ H-NMR spectrum of CyT -----	S4
¹³ C-NMR spectrum of CyT -----	S5
CD spectra of KANA-aptamer in different solution upon addition of KANA -----	S6
UV-vis absorption spectra of CyT upon addition of KANA-aptamer and KANA --	S7
Photographs of samples under UV lamp at different times-----	S8
FL spectra of CyT in different buffer solutions-----	S9
UV-vis absorption spectra of CyT with different K ⁺ concentrations -----	S10
FL spectra of CyT with different KANA-aptamer concentrations in the absence and presence of KANA -----	S11
The reported G-rich sequences of antibiotic aptamers -----	S12
Determination of KANA concentration in lake water and urine by proposed method and standard HPLC-ELSD-----	S13
Comparison with the reported methods for KANA determination -----	S13

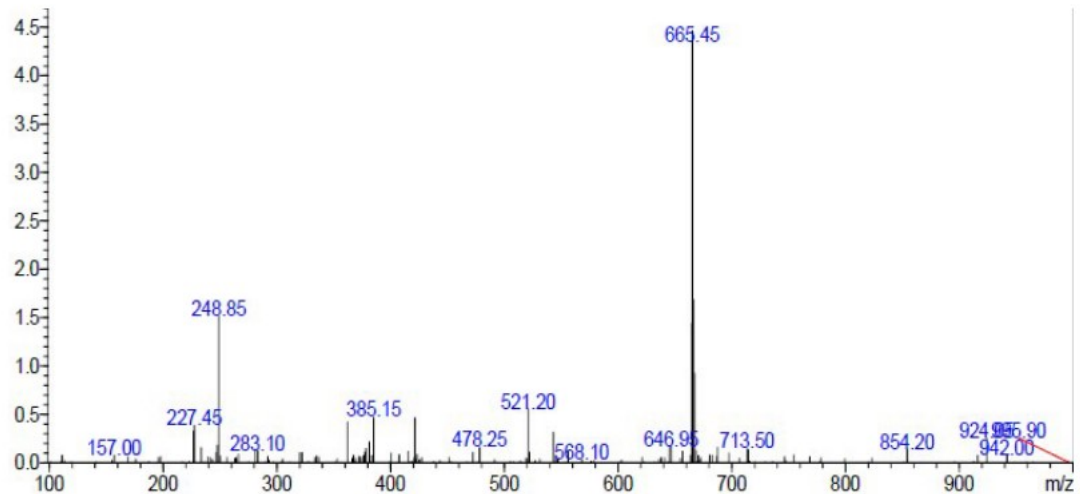


Fig. S1. MS-ESI spectrum of CyT.

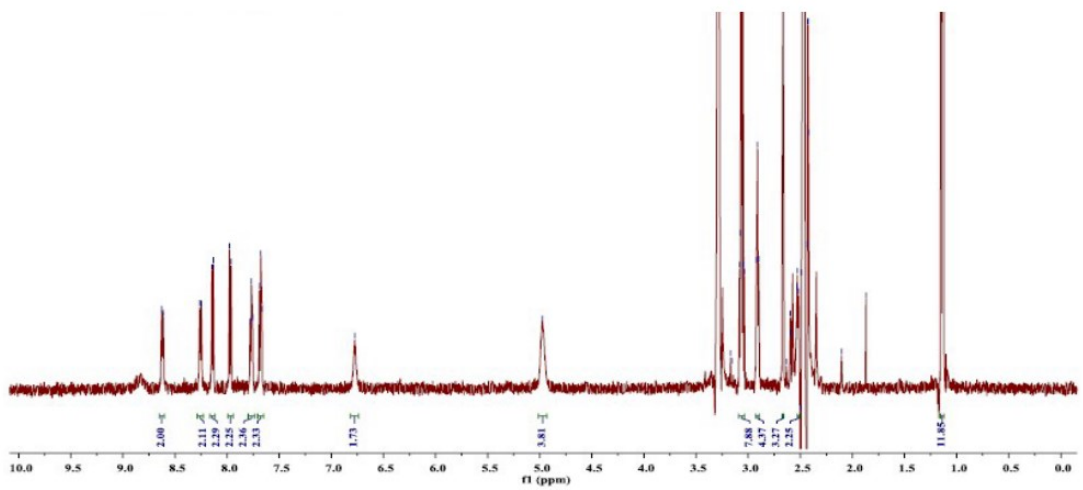


Fig. S2. ¹H-NMR spectrum of cyanine dye CyT in DMSO-d₆. δ ¹H: 8.63–8.61 (d, 2H), 8.26–8.25 (d, 2H), 8.15–8.13 (d, 2H), 7.98–7.96 (d, 2H), 7.77 (t, 2H), 7.68 (t, 2H), 6.78 (s, 2H), 4.97 (s, 2H), 3.06 (m, 8H), 2.91 (t, 4H), 2.67 (s, 3H, CH₃), 2.51 (s, 2H), 1.14 (s, 12H) ppm.

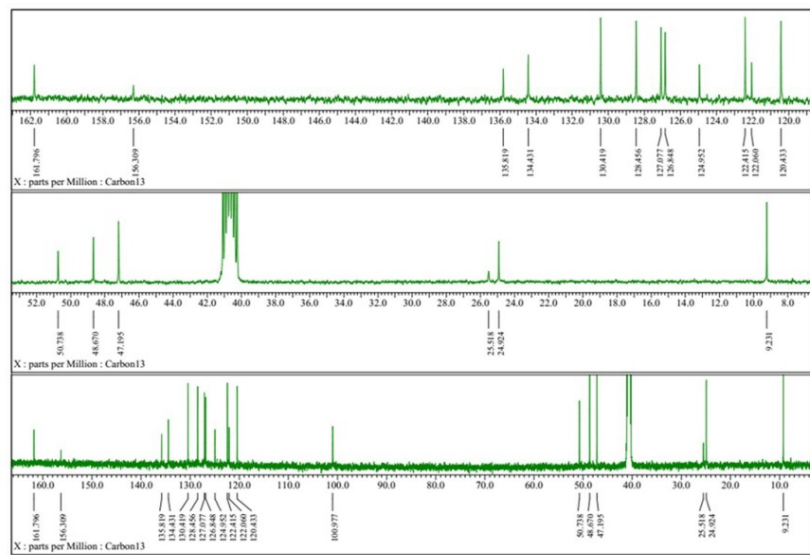


Fig. S3. ^{13}C -NMR spectrum of CyT in DMSO-d6. δ 161.80, 156.31, 135.82, 134.43, 130.42, 128.46, 127.08, 126.85, 124.95, 122.41, 122.06, 120.43, 100.98, 50.74, 48.67, 47.20, 25.52, 24.92, 9.23.

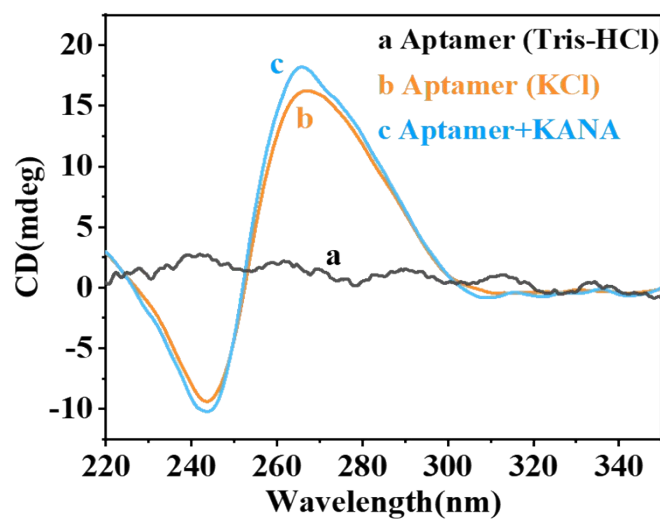


Fig. S4. The CD spectra of (a) KANA-aptamer in 20 mM Tris-HCl, (b) KANA-aptamer in 5 mM KCl, (c) KANA aptamer+KANA in 5 mM KCl. The concentrations of KANA-aptamer and KANA were 3.0 μ M, 0.6 μ M , respectively.

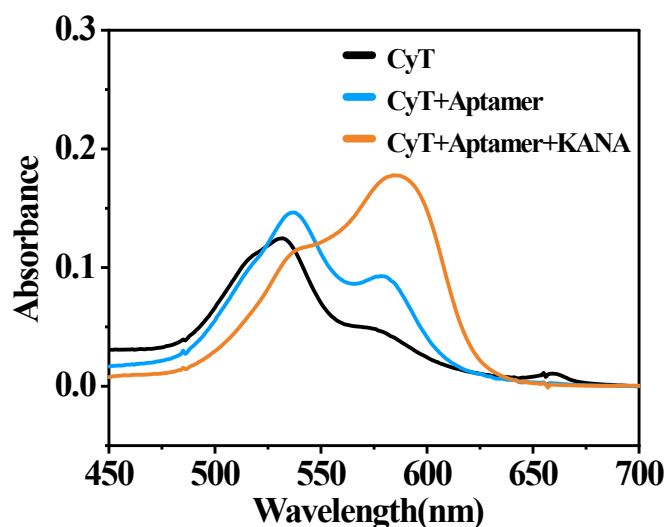


Fig. S5. The absorption spectra of CyT upon addition of KANA-aptamer and KANA. The concentrations of CyT, KANA-aptamer and KANA were 2.0 μM , 2.0 μM , 5.0 μM , respectively.

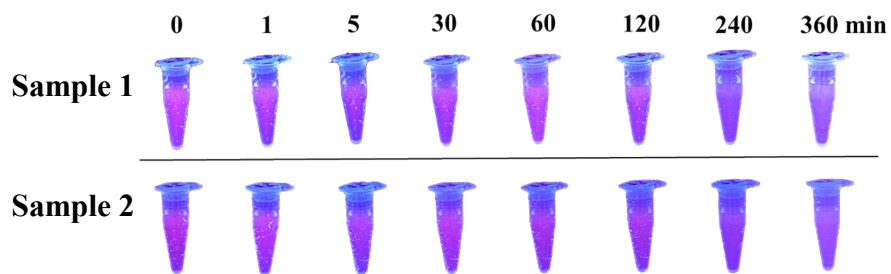


Fig. S6. Photographs of samples under UV lamp (302 nm) at different times. The concentrations of KANA were 0.6 μ M.

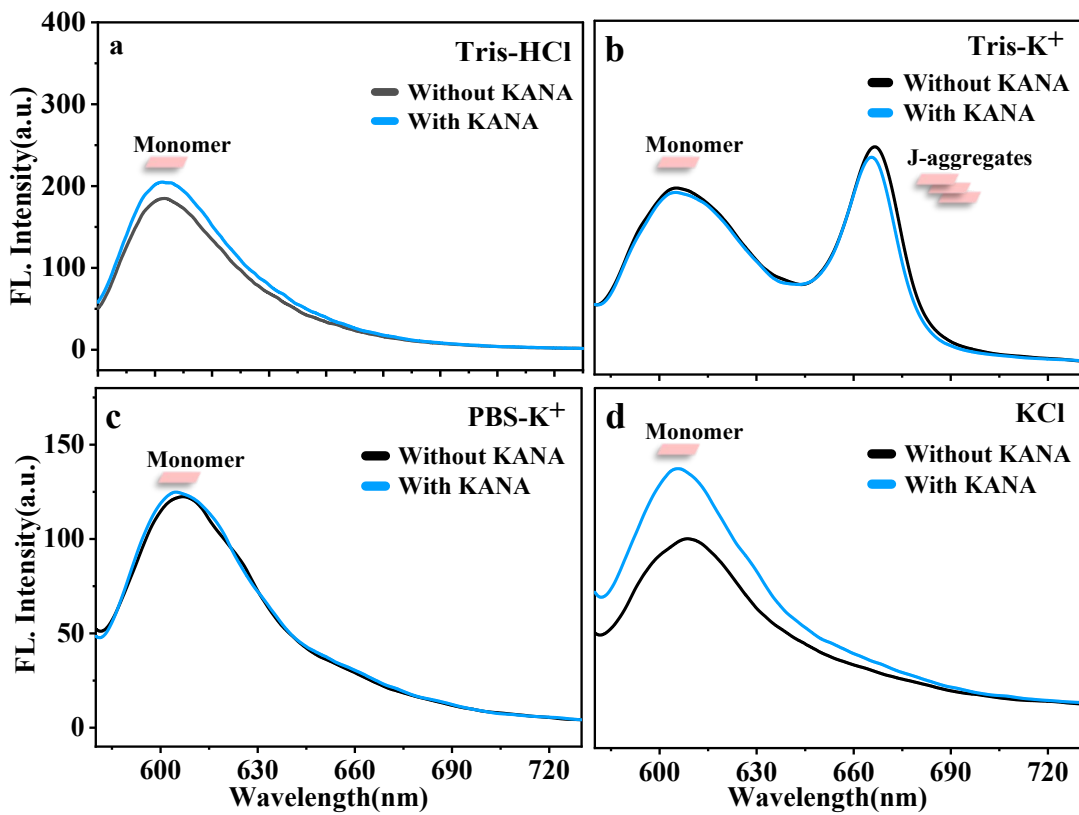


Fig. S7. Fluorescence spectra of CyT in different buffer solutions with (blue) or without (black) KANA ($0.2 \mu\text{M}$). (a) 20 mM Tris-HCl, (b) Tris-K⁺ (20 mM Tris-HCl and 5 mM KCl), (c) PBS-K⁺ (5 mM K⁺), (d) 5 mM KCl.

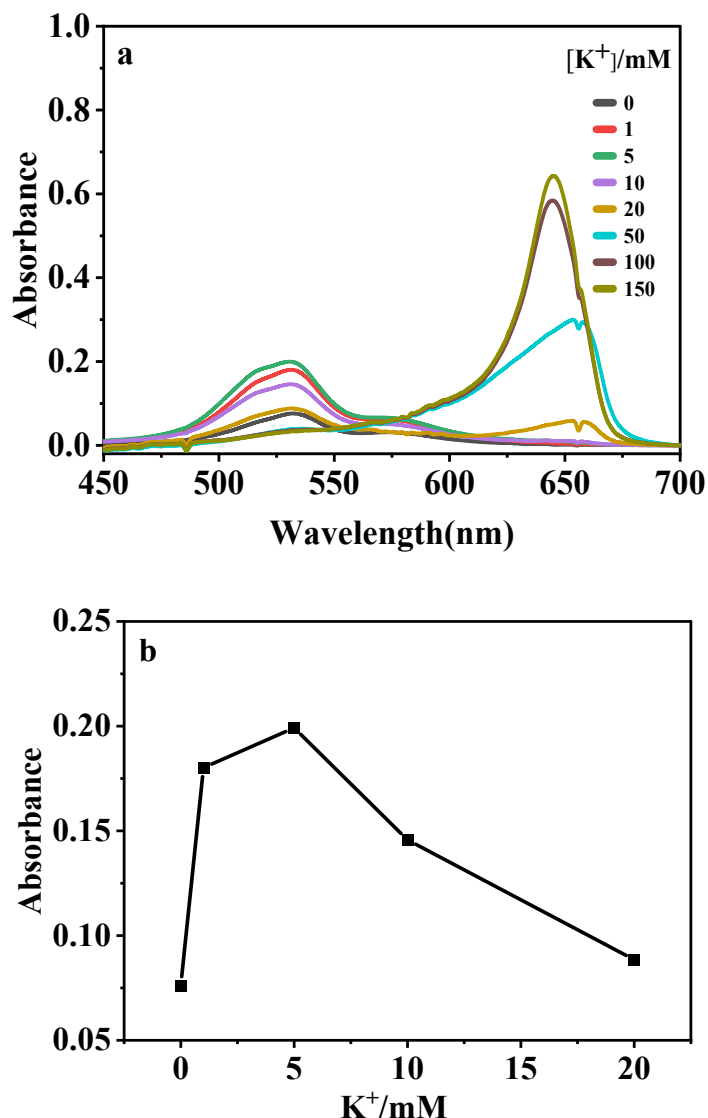


Fig. S8. a) The absorption spectra of 4 μM CyT with increasing concentrations of K⁺. b) The plot of the absorbance at 532 nm of 4 μM CyT versus [K⁺].

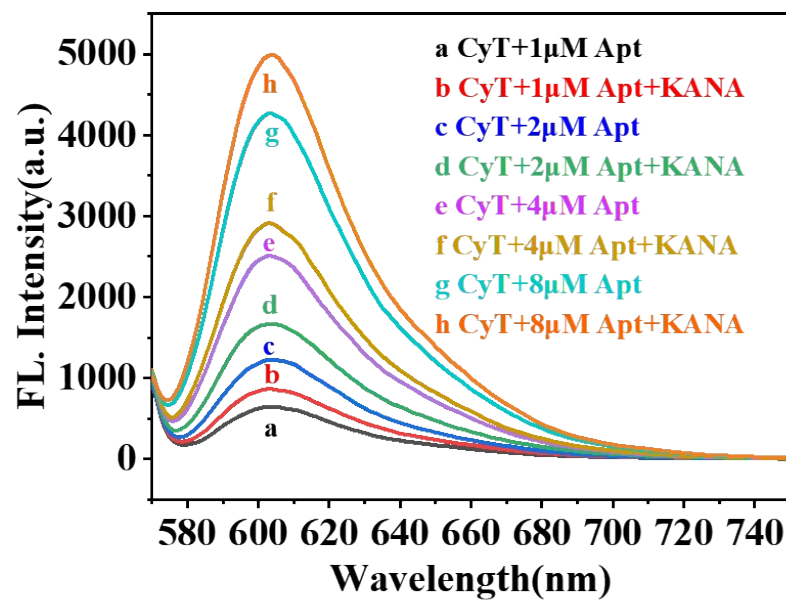


Fig. S9. The fluorescence spectra of 2 μ M CyT with various concentrations of KANA-aptamer in the absence and presence of KANA.

Table S1 The reported G-rich sequence of antibiotic aptamers

Antibiotic Classes	Antibiotics	Aptamer sequence 5'→3'	Confor-mation	Ref.
Tetracyclines	Tetracycline	CGT ACG GAA TTC GCT AGC CCC CCG GCA GGC CAC GGC TTG GGT TGG TCC CAC TGC GCG TGG ATC CGA GCT CCA CGT G TGGGTAGGGCGGGTTGGGA CGGTGGTG	Antiparallel G4	[1]
			-	[2]
	Oxytetracycline	CGTACGGAATTGCTAGCCGAGTTGAGGCCGGCGC GGTACGGGTACTGGTATGTGTGGGGATCCGAGCTC CACGTG	-	[3]
		ATA CCA GCT TAT TCA ATT AGT TGT GTA TTG AGG TTT GAT CTA GGC ATA GTC AAC AGA GCA CGATCG ATC TGG CTTGTT CTA CAA TCG TAA TCA GTT AG	Parallel G4	[4]
Quinolones	Ofloxacin			[5][6]
	Ciprofloxacin			
	Enrofloxacin	CCC ATC AGG GGG CTA GGC TAA CAC GGT TCG GCT CTC TGA GCC CGG GTT ATT TCA GGG GGA TGGGGGTTGAGGCTAAGCGA	G-rich	[7]
Aminoglycosides	Kanamycin	TGGGGGTTGAGGCTAAGCGA	Parallel G4	[8]
		TGG GGG TTG AGG CTA AGC CGA CCA TGT ACT TTT	G-rich	[9]
	Tobramycin	GGG ACT TGG TTT AGG TAA TGA GTC CC GA CTA GGC ACT AGT C	G-rich	[10]
	Gentamicin	GGG ACT TGG TTT AGG TAA TGA GTC CC	G-rich	[11]
Sulfonamides	Streptomycin	GGGGTCTGGTGTCTGCTTGTCTGTCGGGCGT	G-rich	[12]
	Sulfame/thazine	TTA GCT TA T GCG TTG GCC GGG A TA AGG A TC CAG CCG TTG TAG A TT TGC GTT CTA ACT CTC	-	[13]
				[14]
β-Lactams	Ampicillin	GCGGCGGTTGTA TAGCGG	G-rich	[15]
	Penicillin	TTA GTT GGG GTT CAG TTG G	G-rich	[16]
Anthracyclines	Chloramphenicol	GGGTCTGAGGAGTGCAGCGGTGCCAGTGAGT ACT TCA GTG AGT TGT CCC ACG GTC GGC GAG TCG GTG GTA G	G-rich	[17]
			G-rich	[18]

Table S2 Determination of KANA concentration in lake water and urine by proposed method and standard HPLC-ELSD^a

Sample	Proposed method *	HPLC-ELSD *
Lake water	1 Not detected	Not detected
	2 Not detected	Not detected
Urine	1 Not detected	Not detected
	2 Not detected	Not detected

* Average value of three determinations ±standard deviation

^aThe standard HPLC-ELSD method as described in the Chinese pharmacopoeia

Table S3 Comparison with the reported methods for KANA determination

Detection method	LOD	Linear range	Application	Ref.
HPLC	1.23 nM	10-31 μM	-	[19]
ELISA	0.4 nM	0.4-6.0 nM	Fc fusion protein	[20]
CE	0.83 μM	4.0-65 μM	-	[21]
FRET	1.1 μM	4-25 μM	milk	[22]
Fluorescent	1.05 nM	50-2000 nM	pork, chicken, beef	[23]
Electrochemical	0.06 nM	0.1-60 nM	honey	[24]
Electrochemical	0.23 nM	2.5-155 nM	milk	[25]
Luminescence	143 nM	0.2-150 μM	fish	[26]
Colorimetric	0.06 μM	0.1-0.5μM	honey, milk, pork	[27]
Colorimetric	0.68 μM	1-40 μM	milk	[28]
Fluorescent	43 nM	0.1-1μM	lake water, urine	This work

References

- [1] YANG C, BIE J, ZHANG X, et al. A label-free aptasensor for the detection of tetracycline based on the luminescence of SYBR Green I. Spectrochim Acta A Mol Biomol Spectrosc, 2018, 202: 382-388.
- [2] TANG Y, HUANG X, WANG X, et al. G-quadruplex DNAzyme as peroxidase mimetic in a colorimetric biosensor for ultrasensitive and selective detection of trace tetracyclines in foods. Food Chem, 2022, 366: 130560.

-
- [3] LIU S, DING J, QIN W. Dual-Analyte Chronopotentiometric Aptasensing Platform Based on a G-Quadruplex/Hemin DNAzyme and Logic Gate Operations. *Anal Chem*, 2019, 91(4): 3170-3176.
 - [4] ZHAO H, GAO S, LIU M, et al. Fluorescent assay for oxytetracycline based on a long-chain aptamer assembled onto reduced graphene oxide. *Microchimica Acta*, 2013, 180(9-10): 829-835.
 - [5] YI H, YAN Z, WANG L, et al. Fluorometric determination for ofloxacin by using an aptamer and SYBR Green I. *Mikrochim Acta*, 2019, 186(10): 668.
 - [6] HU X, WEI P, CATANANTE G, et al. Ultrasensitive ciprofloxacin assay based on the use of a fluorescently labeled aptamer and a nanocomposite prepared from carbon nanotubes and MoSe₂. *Mikrochim Acta*, 2019, 186(8): 507.
 - [7] CHEN J, JIN Y, REN T, et al. A novel terbium (III) and aptamer-based probe for label-free detection of three fluoroquinolones in honey and water samples. *Food Chem*, 2022, 386: 132751.
 - [8] MA L, SUN N, TU C, et al. Design of an aptamer-based fluorescence displacement biosensor for selective and sensitive detection of kanamycin in aqueous samples. *RSC Advances*, 2017, 7(61): 38512-38518.
 - [9] ZHOU W, XU L, JIANG B. Target-initiated autonomous synthesis of metal-ion dependent DNAzymes for label-free and amplified fluorescence detection of kanamycin in milk samples. *Anal Chim Acta*, 2021, 1148: 238195.
 - [10] MAHJUB R, SHAYESTEH O H, DERAKHSHANDEH K, et al. A novel label-free colorimetric polyA aptasensing approach based on cationic polymer and silver nanoparticles for detection of tobramycin in milk. *Food Chem*, 2022, 382: 132580.
 - [11] OU Y, JIN X, FANG J, et al. Multi-cycle signal-amplified colorimetric detection of tobramycin based on dual-strand displacement and three-way DNA junction. *Microchemical Journal*, 2020, 156: 104823.
 - [12] RAMALINGAM S, COLLIER C M, SINGH A. A Paper-Based Colorimetric Aptasensor for the Detection of Gentamicin. *Biosensors (Basel)*, 2021, 11(2):
 - [13] ZHOU N, WANG J, ZHANG J, et al. Selection and identification of streptomycin-specific single-stranded DNA aptamers and the application in the detection of streptomycin in honey. *Talanta*, 2013, 108: 109-116.
 - [14] HE B, LI M, LI M. Electrochemical determination of sulfamethazine using a gold electrode modified with multi-walled carbon nanotubes, graphene oxide nanoribbons and branched aptamers. *Mikrochim Acta*, 2020, 187(5): 274.
 - [15] ZHANG R, WANG Y, QU X, et al. Exonuclease III-powered DNA Walking Machine for Label-free and Ultrasensitive Electrochemical Sensing of Antibiotic. *Sensors and Actuators B: Chemical*, 2019, 297:
 - [16] MOHAMMAD-RAZDARI A, GHASEMI-VARNAMKHASTI M, IZADI Z, et al. An impedimetric aptasensor for ultrasensitive detection of Penicillin G based on the use of reduced graphene oxide and gold nanoparticles. *Mikrochim Acta*, 2019, 186(6): 372.
 - [17] YU Z, CUI P, XIANG Y, et al. Developing a fast electrochemical aptasensor method for the quantitative detection of penicillin G residue in milk with high sensitivity and good anti-fouling ability. *Microchemical Journal*, 2020, 157: 105077.

-
- [18] WAN HUANGA H Z, GUOSONG LAIA,, SHUN LIUA,BOLIA, AIMIN YU. Sensitive and rapid aptasensing of chloramphenicol by colorimetric signal. *Food Chemistry*, 2019, 270: 287 - 292.
- [19] PATEL K N, LIMGAVKAR R S, RAVAL H G, et al. High-Performance Liquid Chromatographic Determination of Cefalexin Monohydrate and Kanamycin Monosulfate with Precolumn Derivatization. *Journal of Liquid Chromatography & Related Technologies*, 2014, 38(6): 716-721.
- [20] CHANG C Y, CUI Y, LI X R, et al. Determination of kanamycin residues in recombinant human thrombopoietin mimetic peptide-Fc fusion protein for injection by ELISA. *Chinese Journal of Pharmaceutical Analysis*, 2019, 39(2): 328-332.
- [21] ZHU Y, GE S, WU M, et al. Rapid Separation and Determination of Aminoglycoside Antibiotics by Capillary Electrophoresis with Contactless Conductivity Detection. *Physical Testing and Chemical Analysis (Part B:Chemical Analysis)*, 2014, 50(5): 525-529.
- [22] WANG Y, MA T, MA S, et al. Fluorometric determination of the antibiotic kanamycin by aptamer-induced FRET quenching and recovery between MoS₂ nanosheets and carbon dots. *Microchimica Acta*, 2016, 184(1): 203-210.
- [23] WANG C, LI J. Fluorescence method for kanamycin detection based on the conversion of G-triplex and G-quadruplex. *Anal Bioanal Chem*, 2021, 413(28): 7073-7080.
- [24] WANG C, LIU C, LUO J, et al. Direct electrochemical detection of kanamycin based on peroxidase-like activity of gold nanoparticles. *Anal Chim Acta*, 2016, 936: 75-82.
- [25] SHARMA A, ISTAMBOULIE G, HAYAT A, et al. Disposable and portable aptamer functionalized impedimetric sensor for detection of kanamycin residue in milk sample. *Sensors and Actuators B: Chemical*, 2017, 245: 507-515.
- [26] LEUNG K-H, HE H-Z, CHAN D S-H, et al. An oligonucleotide-based switch-on luminescent probe for the detection of kanamycin in aqueous solution. *Sensors and Actuators B: Chemical*, 2013, 177: 487-492.
- [27] TANG Y, HU Y, ZHOU P, et al. Colorimetric Detection of Kanamycin Residue in Foods Based on the Aptamer-Enhanced Peroxidase-Mimicking Activity of Layered WS₂ Nanosheets. *J Agric Food Chem*, 2021, 69(9): 2884-2893.
- [28] XU C, YING Y, PING J. Colorimetric aggregation assay for kanamycin using gold nanoparticles modified with hairpin DNA probes and hybridization chain reaction-assisted amplification. *Mikrochim Acta*, 2019, 186(7): 448.